

**USERS' GUIDE
TO
CAFI**

(**C**omputation of **A**coustic **F**luctuations from **I**nternal waves)

Stanley M. Flatté and Galina Rovner

Physics Department
University of California
Santa Cruz, CA 95064

June 29, 1998

References

- [1] S. Flatté, R. Dashen, W. Munk, K. Watson, and F. Zachariassen, *Sound Transmission Through a Fluctuating Ocean* (A 300 page monograph published by the Cambridge University Press in their series on Mechanics and Applied Mathematics, 1979).
- [2] W. Munk and C. Garrett, "Internal waves in the ocean," *Ann. Rev. Fluid Mech.* **11**, 339–369 (1979).
- [3] S. Flatté and G. Rovner, "Path-integral expressions for fluctuations in acoustic transmission in the ocean waveguide," In *Methods of Theoretical Physics Applied to Oceanography*, P. Müller, ed., pp. 167–174 (Proceedings of the Ninth 'Aha Huliko'a Hawaiian Winter Workshop, 1997).
- [4] R. Dashen, S. Flatté, and S. Reynolds, "Path-integral treatment of acoustic mutual coherence functions for rays in a sound channel," *J. Acoust. Soc. Am.* **77**, 1716–22 (1985).
- [5] S. Flatté, "Wave propagation through random media: Contributions from ocean acoustics," *Proc. of the IEEE* **71**, 1267–1294 (1983).
- [6] R. Esswein and S. Flatté, "Calculation of the phase-structure function density from oceanic internal waves," *J. Acoust. Soc. Am.* **70**, 1387–96 (1981).
- [7] S. Flatté, "Sound transmission through internal waves, including internal wave tomography," in *A Celebration of Geophysics and Oceanography - 1982* (Scripps Institution of Oceanography Reference Series 84-5, 1984).
- [8] S. Flatté and R. Stoughton, "Theory of acoustic measurement of internal-wave strength as a function of depth, horizontal position, and time," *J. Geophys. Res. - Oceans* **91**, 7709–7720 (1986).
- [9] R. Esswein and S. Flatté, "Calculation of the strength and diffraction parameters in oceanic sound transmission," *J. Acoust. Soc. Am.* **67**, 1523–31 (1980).
- [10] S. Flatté and R. Stoughton, "Predictions of internal-wave effects on ocean acoustic coherence, travel-time variance, and intensity moments for very long-range propagation," *J. Acoust. Soc. Am.* **84**, 1414–1424 (1988).

- [11] S. Flatté, S. Reynolds, and R. Dashen, “Path-integral treatment of intensity behavior for rays in a sound channel,” *J. Acoust. Soc. Am.* **82**, 967–972 (1987).
- [12] S. Flatté, D. Bernstein, and R. Dashen, “Intensity moments by path integral techniques for wave propagation through random media, with application to sound in the ocean,” *Phys. Fluids* **26**, 1701–13 (1983).

Contents

1	THEORETICAL INTRODUCTION	3
1.1	General Introduction	3
1.2	The Ocean Sound Channel	3
1.3	Internal Waves	4
1.4	Statistical Quantities of Interest	6
1.5	Ray Geometry	8
2	BRIEF DESCRIPTION OF CAFI INPUT AND OUTPUT	12
3	DETAILED DESCRIPTION OF CAFI INPUT	14
3.1	Parameter File	14
3.2	Sound-Speed Profile File	22
3.3	Buoyancy Frequency Profile File	25
3.4	Fluctuations ($\langle \mu^2 \rangle$) Profile File	28
4	DETAILED DESCRIPTION OF LONG OUTPUT FILE	32
4.1	Example of a long out put file	32
4.2	User - Provided Parameters	37
4.2.1	Source - receiver geometry	37
4.2.2	Numerical accuracy parameters	37
4.2.3	Internal wave parameters	38
4.3	Calculated Parameters	39
4.4	Ray Geometry Quantities	40
4.4.1	Ray turning-point quantities	40
4.4.2	Quantities at range of receiver:	41
4.5	Wave Propagation Region	42
4.6	Space Scales	44
4.7	Frequency Scales (Coherent Bandwidth)	45
4.8	Time Scales	46
4.9	Validity of Path Integral	46
4.10	Microray Focusing Parameter	48
5	DESCRIPTION OF SHORT OUTPUT FILE	50

List of Figures

1	Ray geometry	9
2	Input profiles from AET experiment. These profiles are plots of the data listed for aet.ss, aet.bf, and aet.fl, in Chapters 3.2 to 3.4.	31
3	The three quantities plotted are the rms travel-time (τ), the vertical coherence angle (Θ_v), and the horizontal coherence angle (Θ_h). This plot was made from the information contained in the short output file listed above.	52

1 THEORETICAL INTRODUCTION

1.1 General Introduction

The ocean environment through which sound is transmitted has a complex structure. The result of warming in the upper kilometer at mid-latitudes, and certain principles of water mass formation, is an ocean with a density gradient diminishing strongly with depth. This ocean property underlies both the shape of the ocean sound channel and the depth dependence of internal-wave induced sound-speed fluctuations.[1]

In the geometrical optics approximation, the field transmitted from a source can be described completely in terms of rays, whose characteristics are determined by the sound speed as a function of position. We need the sound-speed profile in order to calculate the trajectories of rays and also the behavior of ray tubes; that is the focusing and defocusing of ray bundles due to the second derivative of the sound-speed profile. Deterministic diffractive effects beyond geometrical optics can be calculated by various wave methods, but no such calculations are done in this code. This code does calculate statistical effects of internal waves: both their effects within the geometrical optics approximation, and their diffractive effects. These internal-wave calculations are done by means of corrections to deterministic ray theory derived from path-integral techniques.[1]

1.2 The Ocean Sound Channel

The most striking feature of ray propagation in the ocean is the sound channel. The sound-speed profile has a minimum at a depth that varies with geographical location, but is typically about 1 km at temperate latitudes, decreasing to zero in the polar regions. Rays tend to bend toward regions of smaller sound speed, and are thereby channeled toward the depth of minimum speed, called the sound axis. As a result, refracted rays may extend for thousands of kilometers in range, never touching surface or bottom. The typical sound-speed profile is a result of the competition between the stratification of the ocean (in temperature and salinity) which tends to give a sound-speed decrease with depth, and the adiabatic pressure gradient which tends to give an increase with depth. The stratification dominates in the upper regions and the pressure gradient dominates in the lower depths.

The most important source of ocean variability on time scales from a few minutes to days is internal waves: ocean gravity waves made possible by the density increase with depth and the restoring force of gravity. The sources of these internal waves are

dynamic disturbances such as surface waves, currents flowing over bottom topography or nonlinear dynamical interactions within the volume of the ocean.

If one ignores other effects, such as mesoscale eddies and fronts, then the field of sound-speed can be expressed as

$$C(\mathbf{x}, t) = C_0[1 + U_0(z) + \mu(\mathbf{x}, t)], \quad (1)$$

where C_0 is a reference sound speed, $C(z) = C_0[1 + U_0(z)]$ is the depth-dependent average sound-speed profile, and $\mu(\mathbf{x}, t)$ is a random, zero-mean fluctuation field caused by internal waves.

1.3 Internal Waves

Ideally, one would like to have measurements of the statistical properties of $\mu(\mathbf{x}, t)$ continuously in all three spatial dimensions and in time. For practical reasons, we rely on the model for the internal-wavefield developed by Garrett and Munk (GM).[2]

The behavior of $\mu(\mathbf{x}, t)$ is determined from the displacement $\zeta(x, t)$ of an isodensity surface due to internal waves by the formula

$$\mu(\mathbf{x}, t) = \zeta(x, t)[\partial_z U_0 - \gamma_A] \quad (2)$$

where γ_A is the adiabatic sound-speed gradient, which is a function of temperature, salinity, and pressure. Internal-wave displacements can be characterized by a distribution over internal-wave modes, yielding, among other quantities, a profile of displacement variance. However, acoustic effects depend on sound-speed fluctuations, and hence the profile of $\langle \mu^2 \rangle$. In certain cases the $\langle \mu^2 \rangle$ profile is available directly. If it is not, a good model of the sound channel U_0 and an accurate calculation of γ_A are needed to produce one.

The dynamics of internal waves restricts the relation between the spatial and temporal behavior of $\zeta(\mathbf{x}, t)$. These restrictions are controlled by the gradient of density in the ocean, which is conveniently measured by the buoyancy frequency $n(z)$ (often called the Brunt-Väisälä frequency). The buoyancy frequency typically varies from 3 cph near the surface to 0.2 cph near the bottom; the fractional rate of decrease diminishes with depth. We need the entire $n(z)$ profile for a complete characterization of internal waves.

Part of the relation between temporal and spatial behavior of internal waves is determined by the dispersion relation, which can be expressed approximately by the

use of one parameter, historically called n_0B . (We will instead use a parameter called α_d .)

The statistical behavior of $\zeta(\mathbf{x}, t)$ is determined by the spectrum of internal waves, which, in the GM model, is determined by two parameters, ζ_0 and j_* . The quantity ζ_0 may be thought of as the rms internal-wave displacement at a depth where the buoyancy frequency is equal to a reference value, n_a . The parameter j_* , sometimes called the “modal bandwidth,” determines the vertical coherence of internal waves.

Given the sound-speed profile, depth and angle of the ray at the source and using approximations for the equation for rays through a variable sound-speed field, we can calculate ray geometry.

Given the above information about internal waves, we can calculate important quantities associated with the effect of internal waves on sound propagation. For example, the variance of fractional sound-speed variations $\langle \mu^2 \rangle$, the vertical correlation length of internal waves L_v , and the internal-wave correlation length along an acoustic ray L_p , are all internal-wave quantities of direct interest for acoustic propagation.[1, 3]

Correlation length, $L_p(\theta, z)$ (“ p ” refers to the correlation length *parallel* to the ray) of the sound-speed fluctuations along the line oriented at angle θ and at depth z is needed for calculations of many statistical properties of the ray. We calculate L_p using empirical formula.[3]

$$L_p = L_{p0} \frac{[1 - \exp[-(\frac{\sigma_c}{\sigma})^p]]^q}{1 + (\frac{\rho_s}{\rho_c})^{q_a} (\frac{\sigma_c}{\sigma})^{p_a}} \quad (3)$$

where $\rho_c, \sigma_c, p, p_a, q, q_a$ are empirical constants: $\rho_c=3.5, \sigma_c=0.0204, p=0.385, p_a=0.5, q=1.3, q_a=2.0$; σ is a dimensionless parameter that represents the ratio between an internal-wave length scale r_i and the ray radius of curvature r at depth z :

$$\sigma = \frac{r_i}{r} \quad (4)$$

A typical value of r_i is 1000 km; $L_{p0}=L_p(\theta = 0)$.

Empirical formula for L_p applies for $\sigma \geq 0.3$. If $\sigma > 0.3$ then the values for $\sigma = 0.3$ are taken.

Our treatment of the ocean medium includes the effects of anisotropy, statistical inhomogeneity, internal-wave spectra and background sound channel.

1.4 Statistical Quantities of Interest

The general character of fluctuations in a wavefield is controlled by two parameters: Φ representing strength and Λ representing size (spatial extent) of inhomogeneities. Thus these two parameters depend on the internal-wave parameters, as well as the geometry of the acoustic propagation case under consideration and the acoustic frequency σ . The regime of sound transmission (e.g. unsaturated or saturated) is dependent on the values of Φ and Λ . (It is important to note that these quantities are single-frequency quantities. Broad-band behavior is not well characterized by them at present.)

Let $\Psi(0)$ be the observed acoustic field at a given reference position, time and acoustic frequency. The coherence of the field is described by second moments[1, 4], of which the most important are:

$$\langle \psi^*(\Delta z)\psi(0) \rangle = \exp\left[-\frac{1}{2}\left(\frac{\Delta z}{z_0}\right)^2\right] \quad (5)$$

$$\langle \psi^*(\Delta y)\psi(0) \rangle = \exp\left[-\frac{1}{2}\left(\frac{\Delta y}{y_0}\right)^{3/2}\right] \quad (6)$$

$$\langle \psi^*(\Delta t)\psi(0) \rangle = \exp\left[-\frac{1}{2}\left(\frac{\Delta t}{t_0}\right)^2\right] \quad (7)$$

$$\langle \psi^*(\Delta\sigma)\psi(0) \rangle = \exp\left[-\frac{1}{2}(\Delta\sigma\tau)^2\right] \exp\left[i\Delta\sigma\tau_1 - \frac{1}{2}(\Delta\sigma\tau_0)^2\right] \quad (8)$$

$$\frac{\langle I(\Delta t)I(0) \rangle}{\langle I^2 \rangle} = 1 + \exp\left[-\left(\frac{\Delta t}{t_I}\right)^2\right] \quad (9)$$

Where the Δ quantities are separation variables from the reference values of space, time and frequency.

Note that $\tau \equiv \Phi/\sigma$ in (8) is the rms travel-time fluctuation of an impulse travelling along the unperturbed ray. The term $\exp[-1/2(\Delta\sigma\tau)^2]$ is equal to $\langle \psi(\sigma)\psi^*(\sigma + \Delta\sigma) \rangle$ if all the microrays were to lie exactly on the unperturbed ray. The additional terms are due to each microray trajectory being displaced from the unperturbed ray; τ_1 represents a shift of the mean arrival time of a pulse, τ_0 describes the pulse spreading due to the differences in arrival times of the different microrays.

Validity of Path Integral.

We must examine the validity of two assumptions made during the path-integral derivations of equations of type (26). The first is homogeneity: we assumed that quantities like $\langle \mu^2(z) \rangle$ were uniform over any ray tube cross section. This breaks down for very long ranges and low frequencies but also it may break down due to a highly structured sound-speed or buoyancy-frequency profile. The second is isotropy: we assume that $L_p(\theta, z)$ represented the effective correlation length for all paths within the ray tube at that point along the ray. This breaks down if the bundle of possible paths around the equilibrium ray experience smaller effective L_p . We estimate the fractional inhomogeneity errors (which we call ϵ_{inhom}) in our calculations of the strength parameter Φ , the coherence time t_0 , and the vertical coherence length z_0 , and require these parameters to be less than unity for validity of the appropriate path-integral formulas. We estimate anisotropy errors by calculating the frequency f_v , below which an effective parameter $\frac{qL_V^2}{LE}$ is less than unity. We calculate three such frequencies in which the weighting of this effective parameter is like Φ , t_0 , or z_0 , respectively.

Microray Focusing Parameter.

The higher moments of intensity are approximately given by

$$\langle I^n \rangle \approx N! \langle I \rangle^N \left[1 + \frac{N(N-1)}{2} \gamma \right] \quad (10)$$

where γ is called the microray focusing parameter.

The detailed statistics of acoustic signal behavior require the calculation of a number of other quantities. Calculations of coherence lengths (z_0 and y_0), coherence times, γ , ϵ_{inhom} , f_v and many other statistics of acoustic signal behavior are described in section 4, where specific outputs are listed.

1.5 Ray Geometry

Rays characteristics are determined by the sound speed as a function of position. The general equation of ray optics for a ray in a depth-dependent sound-speed profile may be expressed as

$$\partial_x \theta = -C^{-1} \partial_z C \quad (11)$$

where θ is the angle of the ray with the horizontal x coordinate and $\partial_x z = \tan \theta$.

Because the sound speed $C(z)$ never varies by more than a few per cent from the reference C_0 , fully refracted rays within the ocean volume never attain angles of more than $\approx 15^\circ$ from the horizontal, a fact important to the parabolic-equation approximation. [1, 5] In the ray approximation this is equivalent to setting $\tan \theta = \theta$, so we can replace (9) by

$$\partial_{xx} z = -C^{-1} \partial_z C \quad (12)$$

Defining a dimensionless function $U_0(z)$ by

$$C(z) = C_0[1 + U_0(z)] \quad (13)$$

we have, for small $U_0(z)$

$$\partial_{xx} z = -U_0'(z) \quad (14)$$

We use equation (12) to numerically integrate a ray from initial starting depth (source depth) and initial angle (θ_0), and assuming the environment to be range-independent.

Each ray begins from the source with a specified angle and traverses the ocean in a periodic manner because our sound-speed profiles depend only on depth. All quantities at any range from the source can be expressed in terms of quantities obtained within the first double loop of the ray: that is, the range between the source and the second time the ray passes through the source depth. (See geometrical figure below.)

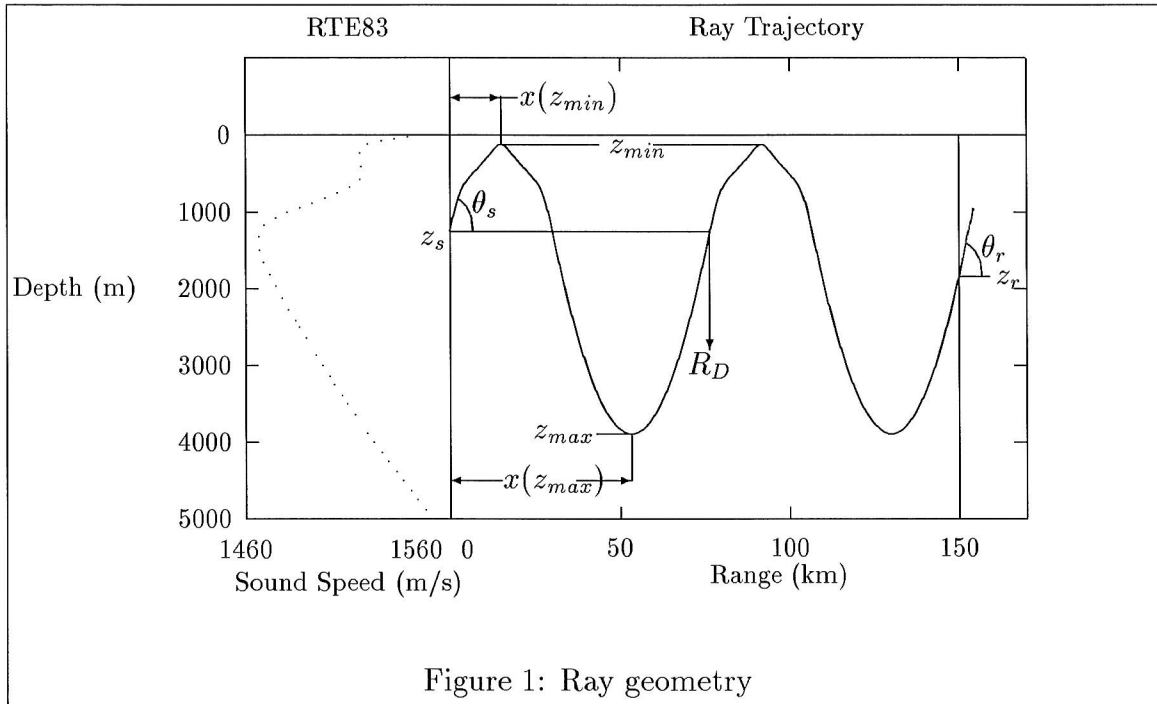


Figure 1: Ray geometry

R_D (m) -double loop length :

the horizontal distance in meters between the acoustic source and the next point on the ray $z(x)$ at which $z = z_0$ and $\theta = \theta_0$

z_{max} :

z coordinate in meters of the ray point farthest from the ocean surface-lower turning point.

$x(z_{max})$:

horizontal distance from the acoustic source to the closest lower turning point.

z_{min} :

z coordinate in meters of the upper turning point or apex.

$x(z_{min})$:

horizontal distance in meters from the acoustic source to apex.

Due to the fluctuation in the ocean the sound signals traveling on the ray are subject to small-angle scatterings by the perturbing potential $V(x)$. The signals thus are slightly deflected from the undisturbed ray in a sort of random walk. When we average over an ensemble of perturbations V the disturbed signals will fill up a

tube surrounding the undisturbed ray. The ray tube behavior is determined by the behavior of the second derivative of U_0 [1, 5].

Consider a ray tube, consisting of nearby rays $z(x)$ surrounding the unperturbed ray $z_{ray}(x)$:

$$z(x) = z_{ray}(x) + \xi(x) \quad (15)$$

Small $\xi(x)$ satisfy the differential equation:

$$\partial_{xx}\xi(x) + U_0''\xi(x) = 0 \quad (16)$$

where the primes in U_0'' mean the derivative with respect to z . Hence properties of ray tubes are controlled by U_0'' .

We define the two solutions of the differential equation (14) by the following boundary conditions:

$\xi_1(x)$ is defined by:

$$\xi_1(0) = 0, \quad \xi_1(R) = 1,$$

$\xi_2(x)$ is defined by:

$$\xi_2(0) = 1, \quad \xi_2(R) = 0,$$

$S_1(x)$ is defined by:

$$S_1(0) = 0, \quad S_1'(0) = 1,$$

$S_2(x)$ is defined by:

$$S_2(0) = 1, \quad S_2'(0) = 0,$$

ξ_1, ξ_2 are needed for Green's functions.

S_1, S_2 is easier to calculate because we have initial conditions for S_1, S_1', S_2, S_2' and can solve different equations.

Consider two ray tubes meeting at x . The Green's function $g(x, x')$, used to represent this situation, satisfies the differential equation

$$\partial_{x'x'}g(x, x') + U_0''g(x, x') = \delta(x' - x) \quad (17)$$

with $g(x, 0) = g(x, R) = 0$. The solution for $g(x, x')$ can be given in terms of the ray tube functions $\xi(x)$ [5] as:

$$g(x, x') = \begin{cases} \xi_1(x')\xi_2(x)S_1(R) & \text{on } (0, x) \\ \xi_1(x)\xi_2(x')S_1(R) & \text{on } (x, R) \end{cases} \quad (18)$$

After a few tens of kilometers from the acoustic source the sound speed field has a rather complicated structure. Several rays from a single source may arrive at a

receiver from different directions, giving rise to multipath. An envelope tangent to a family of rays is called a caustic surface. The Green's function $g(x, x)$ that is used in the definitions of the ray tube and the Fresnel zone goes through infinity at caustics. This happens when $S_1(x) = 0$ so that the boundary conditions cannot be satisfied.

2 BRIEF DESCRIPTION OF CAFI INPUT AND OUTPUT

The execution of the CAFI code is accomplished by a simple command line:

$$cafi < infile > outfile$$

The input to the CAFI program falls into three categories:

1. A parameter file that provides the user with an easy way to vary parameters that are commonly changed, including the names of special input and output files. The name of this file is provided on the command line by the user as the standard input file (*infile* above). The parameters provided by the user in the parameter file fall into several categories:
 - (a) Source-receiver geometry
 - (b) Numerical accuracy parameters
 - (c) Names of files: Sound-speed profile, Buoyancy profile, short output file, long output file
 - (d) Parameters of the internal-wave field.
2. A file to specify the sound-speed profile.
3. A file to specify the buoyancy frequency profile.

The output from the CAFI program falls into three categories:

1. the standard output file (*outfile* above), provided by the user in the command that executes CAFI. This file is used mainly for error and diagnostic messages that are often ignorable.
2. The short output file is created for data that may be used for plotting or other calculational purposes. The contents of that file are determined by coding in the main program code (*driv.f*), and hence could be changed rather easily; however the standard contents of this file are designed to satisfy the interests of most users. (For example, source depth and angle, travel time, transmission loss, rms fluctuation in travel time (τ), etc.)

3. The long output file (if requested) presents the results of CAFI calculations in sections:
 - (a) Ray geometry
 - (b) Definition of wave propagation region (Λ, Φ)
 - (c) Coherence Scales of the acoustic field and the acoustic intensity as a function of Space, Frequency, Time
 - (d) Validity of Path-Integral formula.
 - (e) Microray focusing parameter, γ

3 DETAILED DESCRIPTION OF CAFI INPUT

3.1 Parameter File

The parameter file consists of 17 lines as follows:

```
sfile
bfile
mufile
ffile
lgfile
sdep0,rfin0,rdep0,freq
hseps,hsepr
lat,n0b,gamad
h,hcount
na,jstar,zeta,msqmax
ss,dy,sss,dyy
nflag
yfluct,ylong,yray2
ipl1,nirapl,ipstep,plrang,plstep
nira,angle0,delang
ngrp1 ngrp2 deltaa deltaz
rampmn
wkbjout
```

Here is an example of the parameter file:

```
'../../profiles/aet.ss'    sound speed profile
'../../profiles/aet.bf'    buoyancy frequency profile
'../../profiles/aet.fl'    mu-squred profile
'../../output/aet.650.3Mm' short output,ray geom.,fluct.
'../../long/aet.650.3Mm'   long output
650. 3252382. 1270. 75.    source depth, range, receiver depth,freq
0. 1000.                  hseps, hsepr
25.84 5064. 0.11900e-04    latitude, n0b, adiabatic gradient
10. 20                    h, hcount
3.0000 3.0000 7.300 0.1e-01 na,jstar,zeta,msqmax
```

-10.0 0.0 -10. .01	ss,dy,sss,dyy (sspeed parameters)
21	(nflag =-1 wkbj; =0 n angles; =n>0 ang0+del)
.false. .false.	yfluct(fluct.calc),ylong(write long output)
1 0 2 100000. 400.	plots:1st ray,nu.of plots,ira step,range,plstep
21 -7.5 0.75	number of angles,initial angle, delta angle
40 160 0.00025 10.0	ngrp1,ngrp2(wkbj ray groups),deltaa,deltaz
0.05	min. rel.amplitude from wkbj
'wkbjsv1a400'	wkbj output file

file names *sfile*, *bfile*, *mufile*, *flfile*, *lgfile*, *wkbjout*:

the names of the various files (sound-speed profile, buoyancy-frequency profile, etc.) are any combination of letters and numbers with no blanks between (points and commas can be used) surrounded by single quotes and not exceeding 30 characters including quotes each. These names are relative to current working directory at the time of execution; of course, the full path name can be given instead.

short output file *flfile*:

which has information about each ray at receiver and ray geometry. The first 12 columns give ray geometry information: launch angle, upper turning point depth, range at upper turning point, lower turning point depth, range at lower turning point, double loop length, maximum angle, depth at receiver, angle at receiver, ray identification number, travel time, transmission loss. The next 7 columns (described in detail later) consist of fluctuation parameters and are written only if parameter yfluct (described later) is '.true.' These columns are τ , τ_0 , t_0 , t_I , $\sigma\Lambda$, Θ_h and Θ_v , where the latter two quantities are the rms values of horizontal and vertical tilt of the arriving wavefront.

long output file *lgfile*:

which is designed to be the verbose output file of CAFI, where input parameters and calculated geometrical and internal wave information are printed out in convenient form.

source depth, receiver depth *sdep0*, *rdep0* (units: m) : depth of acoustic source and receiver.

initial angle $angle0$ (units: degrees): angle of ray relative to horizontal, with positive pointing up toward surface.

range $rfin0$ (m) : horizontal distance between acoustic source and receiver.

acoustic frequency $freq$ (Hz) : frequency of the sound signal.

latitude lat (degrees) : average latitude of the source and receiver location.

dispersion relation parameter $n0b$ (cph * m):

n_0B relates the vertical wave number of internal waves to the vertical mode number, as in

$$k_v = \frac{n(z)}{n_0B} \pi j \quad (19)$$

adiabatic gradient $gamad$ (s^{-1}) :

denoted in equations γ_A (for example, eq. (2)), is the adiabatic sound-speed gradient. Since this is a function of temperature, salinity and pressure, we require an average number over the region covered by the ray. It is important that γ_A be less than $\partial_z U_0$ everywhere.

integration step h (m) :

the ray integration step size in meters: horizontal distance used in the numerical integration of the ray equation.

storage step $hcount$:

the storage step size: also we integrate a ray at points spaced in range by h meters, the values at only one out of every $hcount$ points of ray integration are kept in arrays for further usage.

reference buoyancy frequency na (cph) :

reference value used in the definition of the rms displacement of internal waves
The conventional value is 3 cph.

characteristic mode number j_{star} :

denoted in equations by symbol j_* (for example, in eq. (23)), sometimes called the “modal bandwidth” determines the vertical coherence of internal waves. It appears in the expression for the GM spectrum. A commonly used value is $j_* = 3$

rms internal wave displacement ζ (m) :

denoted in equations by ζ_0 , rms internal-wave displacement at depth where buoyancy frequency is equal to a reference value n_a . The variance of internal-wave displacement at depth z is

$$\langle \zeta^2 \rangle = \zeta_0^2 [n_a/n(z)] \quad (20)$$

maximum mu squared $msqmax$:

If $\langle \mu^2 \rangle$ from Eq. (2) exceeds this value, $msqmax$ is used for $\langle \mu^2 \rangle$ instead.

horizontal separation parameters $hseps$, $hsepr$ (m) :

two close-by rays that are straight lines in the horizontal plane have a separation defined by values given at the source and receiver ends.

sound speed profile parameter dy (m) :

sound speed profile is smoothed with a cubic spline technique, (C.H. Reinsch, “Numerische Mathematik,” 1967 (10) 177-183), according to the value of this parameter. It is the rms deviation of the smooth curve from the original data points. If $dy = 0$ then the cubic spline curve goes exactly through the data points - no smoothing is done.

buoyancy frequency profile parameter dyy (cph) :

Buoyancy frequency profile is smoothed with a cubic spline technique, (C.H. Reinsch, “Numerische Mathematik,” 1967 (10) 177-183), according to the value of this parameter. It is the rms deviation of the smooth curve from the original data points. If $dyy = 0$ then the cubic spline curve goes exactly

through the data points - no smoothing is done.

launch angle choice parameter *nflag*:

the flag showing how we wish to choose angles at source for the CAFI run.

We have 3 choices:

- a) *nflag* = -1; b) *nflag* = 0;
- c) *nflag* = *n* > 0 (any integer)

a) *nflag* = -1: In this case part of a program written by M. Brown is run to find the eigen-rays that reach a the given receiver depth at the given range. The initial angles (angles at the source) used in the ray-trace and fluctuation parts of CAFI will be those of the eigen-rays.

b) *nflag* = 0: The program will read an array of initial angles two lines below in the parameter file.

c) *nflag* = *n*: CAFI assumes the input angles are equally spaced, with initial angle and number of angles specified two lines below in the parameter file.

logical variables *yfluct* and *ylong*:

If *yfluct* is .true. then calculations of fluctuation parameters will be done in addition to ray geometry calculations.

If *yfluct* is .false. only ray geometry will be calculated.

If *ylong* is .true. then the 'long' output file will be written;

if *ylong* is .false. the 'long' output file is not written.

The next line in the parameter file is for ray plots. There are several functions of range, calculated by CAFI, that are kept in arrays; the array index represents range in equal increments of $h * hcount$ meters. The subroutine **userpl.f** is available to the user for writing files containing these functions: one file for each ray. The subroutine **userpl.f** can be changed by the user to write any ray variables; the example **userpl.f** provided with CAFI writes a file consisting of lines with two columns: the first is range and the second is depth. This is ideal for making plots of ray trajectories.

There are **5 parameters for ray plots** in this line of the parameter file.

ipl1:

numerical order number of the 1st ray to be plotted, consistent with the order in which CAFI calculations are done for a sequence of rays.

nirapl:

the number of rays to be plotted. If this number is 0 there will be no data files for ray plots written, otherwise, there will be files on the directory from which CAFI is run with names 'ray1', 'ray2', ..., 'raynirapl'. *nirapl* should not be larger than 99.

ipstep:

an integer step for choosing rays for plots: *ipstep* = 1 means make a plot file for each ray.

plrang: the maximum range (in meters) for the ray plot files - can be any number.

plstep: step in range in meters for ray plots. Should be multiples of *hstore*.

The next line of input has to do with the number of angles at source for which CAFI calculations will be done. This line has a variable number of numbers, depending of the value of *nflag* from one of the previous lines. The numbers on this line are:

For the case *nflag* = -1: Only one number is used.

number-of-angles *nira*: can be 0;

if *nira* = 0, then CAFI calculations will be done for all eigen-rays.

If *nira* is positive integer *n*, only *n* angles at the source are chosen: those that correspond to the *n* eigen-rays with the largest relative amplitudes. (Note the parameter *rampmn* defined later allows a restriction to rays above a certain defined amplitude.) The rays that are found under this case are sorted by travel time for the following CAFI calculations. If *n* exceed the number of eigen-rays, CAFI calculations will be done for all eigen-rays.

For the case *nflag* = 0:

number-of-angles *nira*: must be non-zero.

The next n numbers in this line are the specific initial angles desired for the CAFI calculations. These numbers can be negative, positive or 0.0 and they are values of the angle at the source in degrees.

For the case $nflag = -n$: Only three numbers are used.

number-of-angles: must be non-zero.

initial-angle is the first angle (at the source) for which the calculations will be done.

delta-angle is the interval between subsequent angles; the angle will be incremented until **number-of-angles** runs will have been done. To do calculations for a single angle, **number-of-angles** should be 1 and **delta-angle** can be any number.

The next line and all lines below are needed only in case $nflag = -1$, and will be ignored by the program in other cases. This next line contains four numbers, first two of which are ray group numbers as defined by M. Brown in his article. These numbers are related to ray identifier numbers involving the number of upper and lower loops of a ray trajectory. The third number is δa parameter in `wkbj` program, the fourth is δz spacing in depth between the sound-speed profile points in `wkbj`. The `wkbj` part of CAFI, which searches for rays, will restrict its search to rays whose ray group numbers lie on or between these two numbers.

ray-group numbers $ngrp1$, $ngrp2$:

$ngrp1$ is the starting ray-group number. It is safest to set it to zero, but a larger number will save computer time if it is known that no eigenrays have ray-group numbers below a given value. This is the case for long ranges which must contain many double loops.

$ngrp2$ is the ending ray-group number. One can guess what the maximum number needed from an idea of the double-loop length and the range; then $ngrp2$ should be set larger than twice the range divided by the double-loop length. One should do a test to check that no rays are found with larger $ngrp$ numbers.

wkbj parameters δa , δz :

δa is step in ray parameter a in computation of arrival patterns in Michael Brown's `wkbj` program, which is used, optionally, as part of the CAFI system.

deltaz (m) is the vertical spacing between the points in the sound-speed profile in **wkbj**.

minimum relative amplitude *rampmn*:

is the minimum relative amplitude from the wkbj code for rays to be chosen for CAFI calculation - all rays with amplitude smaller than *rampmn* will be excluded.

file name *wkbjout*:

the name of the wkbj output file. This name should not be longer than 30 characters, single quotes included. (See the description of *sfile*.)

All other parameters required by CAFI are compiled into the source code; they are printed out in the 'long' output file and described in Section 3.2.

All data which are on the same line are separated by blanks (not commas).

3.2 Sound-Speed Profile File

The following lines contain an example of the sound-speed-profile file called **sfile**:

Received from John Colosi May 2 1997 Range=3252.382km source depth 650m,
lat 31.03417deg rec.depth 1270m, rec.lat. 20.65067deg (av.lat 25.84deg),
dcdz(potential) in 'dcdzpaet597'. AET sound speed profile

```
aet.ss
357.0
0.1
357
0.00000
5115.00000
1.0
1.0
(f11.6,f12.6)
0.000000 1525.228658
5.000000 1525.325110
10.000000 1525.386438
15.000000 1525.512532
20.000000 1525.603079
25.000000 1525.701895
...
...
180.000000 1513.586711
185.000000 1512.853441
190.000000 1512.081977
195.000000 1511.268409
200.000000 1510.419719
205.000000 1509.544327
...
...
970.000000 1481.585168
980.000000 1481.650900
990.000000 1481.716328
1000.000000 1481.781138
1020.000000 1481.908337
```

```
1040.000000 1482.033406
...
...
2600.000000 1499.602576
2620.000000 1499.911787
2640.000000 1500.222217
2660.000000 1500.533840
2680.000000 1500.846628
...
...
3000.000000 1505.987342
3020.000000 1506.315709
3040.000000 1506.644765
3060.000000 1506.974508
...
...
4980.000000 1540.683511
5000.000000 1541.056540
5020.000000 1541.433388
5040.000000 1541.813541
5060.000000 1542.196280
5080.000000 1542.580880
5100.000000 1542.966622
5115.000000 1543.256244
```

Lines 1-3 contain information about the experiment and (or) some notes about the data. These lines can be left blank.

Line 4 is an experiment identifier string to be printed in the 'long' output file; it can be anything, but a suggestion is that it be the name of the sound-speed data file 'sfile'. All the rest of the file is required for calculations.

Line 5 is the numerical accuracy parameter *ss* (see 4.1.2 for description). The value of *ss* contained in *sfile* will be used only if the *ss* value in the parameter file is negative; otherwise the value in the parameter file supersedes the value in *sfile*.

Line 6 is the numerical accuracy parameter dy (see 4.1.2 for detailed description). The value of dy contained in `sfile` will be used only if the dy value in the parameter file is negative; otherwise the value in the parameter file supersedes the value in `sfile`.

Line 7 is number of data points in this file, which is the number of lines from line 13 to the end of the file.

Line 8 is the minimum depth (0.0 = ocean surface).

Line 9 is the maximum depth in meters, it should be less or equal to the number in the last line of the file in the first column.

Line 10 is the conversion factor for the depth; the depth data in the first column of lines 13 through the last line below are *multiplied* by this conversion factor to obtain the depth in meters, used in CAFI.

Line 11 is the conversion factor for sound-speed; the sound-speed data in the second column of lines 13 through the last line below are *multiplied* by this conversion factor to obtain the sound-speed in meters per second, used in CAFI.

Line 12 is the format in which the data in lines 13 through the last are written.

Lines 13 through the last line of the file are data: 1st column is the depth , 2nd column is corresponding sound speed. It is not required that the data be equally spaced; it is advisable that for the upper 400-500 meters, where the sound speed changes rapidly, the space in depth should be 10-20 meters. For depths over 1500 meters, where the sound speed changes very slowly, the separation of data in depth can be 100 meters or more.

3.3 Buoyancy Frequency Profile File

The following lines contain an example of the file containing the buoyancy frequency information, called **bfile**:

```
Received from John Colosi May 2 1997 Range=3252.382km
source depth 650m, lat 31.03417deg rec.depth 1270m, rec.lat. 20.65067deg
(av.lat 25.84deg),dcdz(potential) in 'dcdzpaet597'. AET buoyancy frequen.
aet.bf
340.0
0.25
340
0.00000
4290.00000
1.0
6.28319
(f11.6,f12.8)
0.000000 0.00000000
5.000000 0.84664863
10.000000 1.56505239
15.000000 2.85966682
20.000000 3.29179358
25.000000 3.66560459
30.000000 3.70680499
35.000000 3.45686936
40.000000 3.39252329
...
...
185.000000 5.77632236
190.000000 5.73974848
195.000000 5.69927645
200.000000 5.64694500
...
...
490.000000 2.60256100
495.000000 2.58320427
500.000000 2.56531096
```

```
510.000000 2.53937697
520.000000 2.50195217
530.000000 2.47888660
...
...
980.000000 1.36245286
990.000000 1.35380852
1000.000000 1.34346318
1010.000000 1.33491886
...
...
2990.000000 0.49526969
3010.000000 0.49573639
3030.000000 0.47854078
3050.000000 0.45885596
3070.000000 0.45896760
...
...
4170.000000 0.22599965
4190.000000 0.21695882
4210.000000 0.20879042
4230.000000 0.18188728
4250.000000 0.16550890
4270.000000 0.15772504
4290.000000 0.18218410
```

Lines 1-3 contain information about the experiment and (or) some notes about the data. These lines can be left blank.

Line 4 is an experiment identifier to be printed in the 'long' output file; it can be anything, but a suggestion is that it be the name of buoyancy frequency data file 'bfile'. All the rest of the file is required for calculations.

Line 5 is the numerical accuracy parameter *sss* (see 4.1.2 for description). The value of *sss* contained in *bfile* will be used only if the *sss* value in the parameter file is negative; otherwise the value in the parameter file supersedes the value in *bfile*.

Line 6 is the numerical accuracy parameter dyy (see 4.1.2 for detailed description). The value of dyy contained in `bfile` will be used only if the dyy value in the parameter file is negative; otherwise the value in the parameter file supersedes the value in `bfile`.

Line 7 is number of data points in this file, which is the number of lines from line 13 to the end of the file.

Line 8 is the minimum depth (0.0 = ocean surface).

Line 9 is the maximum depth in meters, it should be less or equal to the number in the last line of the file in the first column.

Line 10 is the conversion factor for the depth; the depth data in the first column of lines 13 through the last line below are *multiplied* by this conversion factor to obtain the depth in meters, used in CAFI.

Line 11 is the conversion factor for buoyancy frequency; the buoyancy-frequency data in the second column of lines 13 through the last line below are *multiplied* by this conversion factor to obtain the buoyancy frequency in radians per hour, used in CAFI. Thus if the data is provided in cycles/hr, the conversion factor should be $6.28319 (2\pi)$.

Line 12 is the format in which the data in lines 13 through the last are written.

Lines 13 through the last line of the file are data: 1st column is the depth, 2nd column is corresponding buoyancy frequency. It is not required that the data be equally spaced; it is advisable that for the upper 400-500 meters, where the buoyancy frequency changes rapidly, the space in depth should be 10-20 meters. For depths over 1500 meters, where the buoyancy frequency changes very slowly, the separation of data in depth can be 100 meters or more.

3.4 Fluctuations ($\langle \mu^2 \rangle$) Profile File

The following lines contain an example of the $\langle \mu^2 \rangle$ profile file called **mufile**:

```
Received from John Colosi May 2 '97. AET experiment
Range=3252.382km source depth 650m, rec.depth 1270m, (av.lat 25.84deg),
dcdz(potenti) in 'dcdzpaet597' and aet.ss aet.bf used for this musq prof.
aet.fl
000.0
340.0
0.0
341
0.00000
4290.00000
1.0
1.0
(f11.6,e14.6)
0.000000 0.000000E+00
5.000000 0.607428E-10
10.000000 0.325866E-10
15.000000 0.630556E-10
20.000000 0.913506E-10
25.000000 0.167436E-09
30.000000 0.250404E-09
35.000000 0.504002E-09
40.000000 0.978159E-09
45.000000 0.188733E-08
50.000000 0.239662E-08
55.000000 0.276395E-08
...
...
510.000000 0.282141E-07
520.000000 0.244884E-07
530.000000 0.228358E-07
540.000000 0.205588E-07
...
...
```

```

1550.000000 0.398753E-08
1570.000000 0.374936E-08
1590.000000 0.372593E-08
1610.000000 0.384339E-08
...
...
3510.000000 0.142146E-09
3530.000000 0.159977E-09
3550.000000 0.174037E-09
...
...
4230.000000 0.271131E-10
4250.000000 0.246736E-10
4270.000000 0.271970E-10
4290.000000 0.344580E-10

```

Lines 1-3 contain information about the experiment and (or) some notes about the data. These lines can be left blank.

Line 4 is an experiment identifier string it can be anything, but a suggestion is that it be the name of the $\langle \mu^2 \rangle$ data file 'mufile'.

Lines 5 and 6 are the numerical accuracy parameters, as in the sound-speed and buoyancy frequency profile files .

Line 7 is number of data points in this file, which is the number of lines from line 13 to the end of the file.

Line 8 is the minimum depth (0.0 = ocean surface).

Line 9 is the maximum depth in meters, it should be less or equal to the number in the last line of the file in the first column.

Line 10 is the conversion factor for the depth; the depth data in the first column of lines 13 through the last line below are *multiplied* by this conversion factor to

obtain the depth in meters, used in CAFI.

Line 11 is the conversion factor for $\langle \mu^2 \rangle$; the $\langle \mu^2 \rangle$ data in the second column of lines 13 through the last line below are *multiplied* by this conversion factor. Line 11 is, usually, 1.00

Line 12 is the format in which the data in lines 13 through the last are written.

Lines 13 through the last line of the file are data: 1st column is the depth, 2nd column is corresponding $\langle \mu^2 \rangle$. It is not required that the data be equally spaced; it is advisable that for the upper 400-500 meters, the space in depth should be 5-10 meters. For depths over 1500 meters the separation of data in depth can be 20 meters or more.

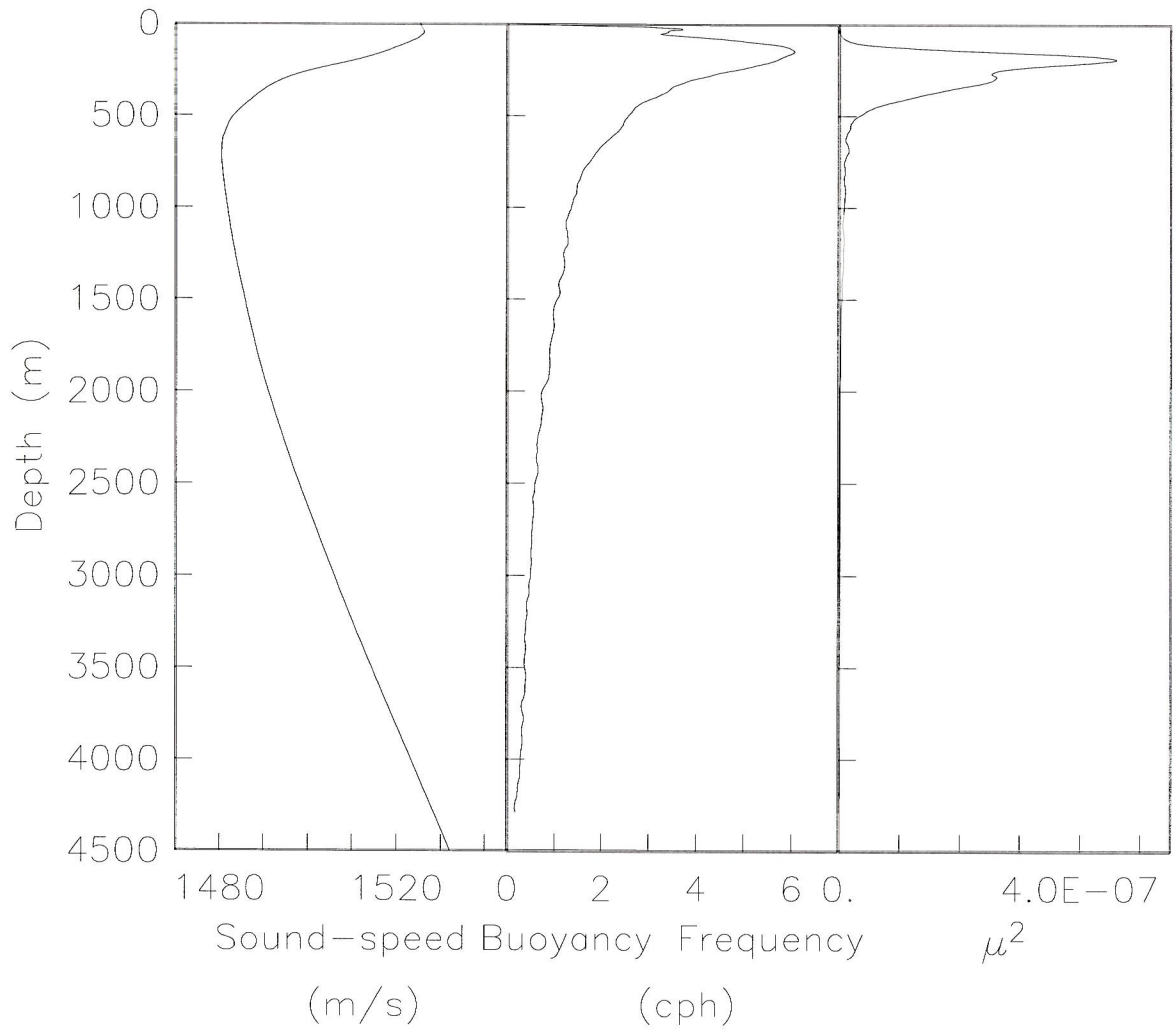


Figure 2: Input profiles from AET experiment. These profiles are plots of the data listed for aet.ss, aet.bf, and aet.fl, in Chapters 3.2 to 3.4.

4 DETAILED DESCRIPTION OF LONG OUT-PUT FILE

4.1 Example of a long out put file

start of run 21 Jan 98 15 48 24

USER-PROVIDED PARAMETERS

Source-receiver geometry

source depth	650.00	m
initial angle	7.0000	deg
range	0.32524E+07	m
receiver depth	1270.0	m

Numerical accuracy parameters

ray integration step size	10.000	m
---------------------------	--------	---

aet597s sound speed profile parameters

ss	smoothing parameter	357.00	
dy	std. dev. of data	0.	m/sec

aet597b buoyancy frequency profile parameters

sss	smoothing parameter	340.00	
dyy	std dev of data	0.10000E-01	

internal wave parameters

na	reference buoyancy frequency	3.0000	cyc/hr
n0b	dispersion relation parameter	5064.0	m-cph
jstar	characteristic mode number	3.0000	
zeta	rms int. wave displacement	7.3000	

gamma	adiabatic gradient	0.11190E-04
latitude		25.840 deg

acoustic frequency		75.000 hz
--------------------	--	-----------

CALCULATED PARAMETERS

storage step size		200.00 m
reference sound speed		1480.4 m/sec
inertial frequency		0.36322E-01 cyc/hr
acoustic wave number		0.31831 1/m
msqmax	maximum mu squared	0.10000E-01
mj		5.3406
njinv		0.46804
avj	<1/j>	0.40006

cpu sec elapsed to trace ray = 0.81667

ray geometry quantities

maximum range integrated	46695.	m
maximum depth reached	2045.8	m
range of maximum depth	27450.	m
minimum depth reached	335.37	m
range of minimum depth	4100.0	m
maximum angle	7.0323	deg
range of maximum angle	46170.	m
depth of maximum angle	714.74	m

ray turning-point quantities

sound speed	1491.7	m/sec
sound speed 1-st derivative	-0.72878E-01	1/sec
u-zero double prime	0.53984E-06	1/(m sq)
mu squared	0.21546E-06	
vertical correlation length	196.10	m

quantities at range of receiver:

ray depth		2008.0	m					
ray angle		1.4644	deg					
travel time		2195.0	sec					
number of loops		69						
min number of iterations		14						
caustics		locations (km)						
139		6.6	48.4	57.2	95.9	107.0	143.8	
152.6	192.0	203.9	235.3	250.7	283.5	297.8	331.7	
345.1	375.1	392.7	423.4	440.4	471.6	488.2	519.9	
536.0	563.2	584.0	611.4	632.0	659.7	680.0	703.1	
723.1	751.4	771.2	799.6	819.3	843.0	867.4	891.3	
910.6	939.5	958.7	982.9	1006.9	1031.2	1050.1	1079.4	
1098.3	1122.8	1146.5	1171.1	1194.8	1219.3	1238.0	1262.7	
1286.2	1311.0	1334.4	1359.2	1377.7	1402.6	1425.9	1450.9	
1474.2	1499.1	1522.4	1542.5	1565.7	1590.9	1613.9	1639.1	
1662.2	1687.4	1705.5	1730.8	1753.7	1779.0	1802.0	1827.3	
1845.3	1870.7	1893.5	1918.9	1941.8	1967.2	1985.1	2010.6	
2033.4	2058.8	2081.6	2107.1	2129.9	2150.5	2173.2	2198.7	
2221.5	2247.0	2269.8	2290.4	2313.1	2338.7	2361.3	2386.9	
2409.6	2430.3	2452.9	2478.6	2501.2	2526.8	2549.5	2570.2	
2592.8	2618.5	2641.0	2666.7	2689.3	2710.1	2732.6	2758.4	
2780.9	2806.6	2829.2	2850.0	2877.5	2898.4	2920.8	2946.6	
2969.1	2994.9	3017.4	3038.3	3060.7	3086.5	3109.0	3134.8	
3157.2	3178.2	3200.5	3226.4	3248.8				
rfrac=amod(rfinal,rmax)		30402.	m					
s1		-65622.398						
s2		-2.0248630						
t1	transmission loss	113.29253						

cpu sec to calculate geometrical information = 0.83333E-01

cpu sec to calculate tau integrals = 0.16667E-01

WAVE PROPAGATION REGION

This ray is tentatively identified as being fully saturated

phi	=	6.6023	lambda	=	0.37995
lambda phi	=	2.5085	lambda phi square	=	16.562
ln(phi)	=	1.8874			

The micropaths are spread over a vertical distance ($\lambda \phi L_v$) of 491.91 m
The approximate number of micropaths or the rms phase difference between one micropath and another ($\lambda \phi^2$) is 16.562

cpu sec to calculate wave region = 1.8833

SPACE SCALES

vertical coherence wavenumber	= kv	= 0.28765E-01	1/m
vertical coherence length	= 1/kv	= 34.765	m
rms vertical-angle spread	= kv/q	= 5.1780	deg
horizontal decorrelation	= pkhsq	= 4.6881	no units
rms horizontal-angle spread	= thh	= 0.38977	deg

cpu sec to calculate space scales = 0.13333

FREQUENCY SCALES (Coherent Bandwidth)

derivative of Q phase at zero frequency	= tau1	= -33.042	millisec
second derivative of Q (square root) (controls pulse spread)	= tau0	= 22.412	millisec
coherent bandwidth	= 1/tau0	= 44.620	Hz

cpu sec to calculate frequency scales = 0.16667E-01

TIME SCALES

rms pulse time jitter	= tau	= 14.010	ms
effective acoustic overall phase time scale	= t0	= 5.9195	minutes
effective internal wave time scale	= phi*t0	= 0.65137	hr
intensity time scale	= ti	= 1.7333	minutes

cpu sec to calculate time scales = 0.

VALIDITY OF PATH INTEGRAL

The following parameters should be less than unity
for validity of the appropriate path-integral formulas:

	ANISOTROPY	INHOMOGENEITY
phi	0.51468	-0.62951
second moment (time)	0.33091	-0.88121
second moment (vert. separ.)	0.26813	-0.93798

cpu sec to calculate validity of path integral= 0.

CORRECTION TO SCINTILLATION INDEX

full calculation

gamma = 0.67865E-01

cpu secs to calculate gamma = 0.71667

cpu sec elapsed to do all ray calculations = 4.1667

end of run 21 Jan 98 15 48 27

4.2 User - Provided Parameters

4.2.1 Source - receiver geometry

source depth
initial angle
range
receiver depth

For detailed description of above parameters see **3.1**

4.2.2 Numerical accuracy parameters

ray integration step size h
sound speed profile parameter dy
buoyancy frequency profile parameter dyy

For detailed description of above parameters see **3.1**

Storage step size $h * hcount$:

due to the limitation on computer storage size and for time efficiency of the program only one out of every $hcount$ points of the calculated functions are stored for further usage. We use array size 1000.

4.2.3 Internal wave parameters

reference buoyancy frequency n_a :

reference value used in the definition of the rms displacement of internal waves
The conventional value is 3 cph.

dispersion relation parameter $n_0 b$:

$n_0 B$ relates the vertical wave number of internal waves to the vertical mode number [6, 7], as in

$$k_v = \frac{n(z)}{n_0 B} \pi j$$

if k_v is small = internal waves are coherent electrically - you get bias don't get spread in the pulse.

characteristic mode number j_{star} :

j_* sometimes called the "modal bandwidth" determines the vertical coherence of internal waves. It appears in the expression for the GM spectrum. A commonly used value is $j_* = 3$.

only when j is large we have bias and

rms internal wave displacement ζ_0 (m):

ζ_0 is the rms internal-wave displacement at depth where buoyancy frequency is equal to a reference value n_a . The variance of internal-wave displacement at depth z is [7]:

$$\langle \zeta^2 \rangle = \zeta_0^2 [n_a/n(z)] \quad (22)$$

maximum mu squared msq_{max} :

If $\langle \mu^2 \rangle$ from Eq. (2) exceeds this value, msq_{max} is used for $\langle \mu^2 \rangle$ instead.

adiabatic gradient γ_A (s^{-1}):

γ_A is the adiabatic sound-speed gradient [1]. Since this is a function of temperature, salinity and pressure, we require an average number over the region covered by the ray. It is important that γ_A be less than $\partial_z U_0$ everywhere.

latitude lat (degrees): average latitude of the source and receiver location.

acoustic frequency $freq$ (Hz): frequency of the sound signal.

4.3 Calculated Parameters

inertial frequency ω_i (cph):

$$\omega_i = 2\Omega \sin(\text{latitude}) \quad (23)$$

ω_i is inertial (or Coriolis) frequency, Ω is the Earth's angular velocity.

reference sound speed c_0 (m s^{-1}):

$$C_0 = \min[C(z)] \quad (24)$$

where $C(z)$ is the sound-speed profile used for calculations.

acoustic wave number q_0 (m^{-1}):

reference wave number of sound signal

$$q_0 = 2\pi \cdot \text{freq} / C_0 \quad (25)$$

where C_0 is the reference sound speed.

mj, njinv, avj:

sums needed for further calculations. They are used in different formulas and are calculated using analytical expression[6]:

$$\text{mj} \equiv M_j, M_j^{-1} \equiv \sum_{j=1}^{\infty} \frac{1}{j(j^2 + j_*^2)} = \frac{1}{j_*^2} \cdot (\gamma_E + \ln j_* + \frac{1}{12 \cdot j_*^2} + \frac{1}{120 \cdot j_*^4}) \quad (26)$$

$$\text{njinv} \equiv N_j^{-1} \equiv \sum_{j=1}^{\infty} \frac{1}{(j^2 + j_*^2)} = \frac{\pi}{2j_*} \cdot \coth(\pi \cdot j_*) - \frac{1}{2 \cdot j_*^2} \quad (27)$$

$$\text{avj} \equiv \langle \frac{1}{j} \rangle = \frac{N_j}{M_j} \quad (28)$$

where j is vertical mode number.

large j will diffuse
wave front much
more, than
small j

4.4 Ray Geometry Quantities

maximum range integrated: one double loop length R_D (see figure 1).

maximum depth reached:
 z_{max} (see figure 1).

range of maximum depth:
 $x(z_{max})$ (see figure 1).

minimum depth reached:
 z_{min} (see figure 1).

range of minimum depth:
 $x(z_{min})$ (see figure 1).

maximum angle:
ray has the largest angle with the horizontal at the sound axis, with the ray pointing up.

range of maximum angle
horizontal distance x in meters from the acoustic source to the point where the ray crosses the sound axis pointing upward.

depth of maximum angle
 z coordinate of the ray's maximum angle point (sound axis depth).

4.4.1 Ray turning-point quantities

The quantities listed below are evaluated at the ray apex, (upper turning point) and are useful because many fluctuation quantities are dominated by contributions near the apex[1, 8].

sound speed:
sound speed at the apex, calculated using the input sound-speed profile, sound-speed profile parameters dy and ss and cubic spline technique.

sound speed 1st derivative:

first derivative of the sound speed at apex calculated quantity; the ray geometry is controlled by the first derivative of C .

u-zero double prime:

value of U_0'' at the apex.

mu squared:

$$\text{musq} = \langle \mu^2(z = z_a) \rangle \quad (29)$$

$\langle \mu^2(z) \rangle$ is the variance of the internal wave sound-speed fluctuations $\mu(x, t)$ as a function of depth. μ is a random, zero mean contribution to the sound-speed field $C(x, t)$ caused by internal waves [see Eq. (1)]. The internal wave model[2] predicts the depth dependence of the variance of μ to be:

$$\langle \mu^2(z) \rangle = \zeta_0^2 [n_a/n(z)] (C^{-1} \partial_z C - \gamma_A)^2 \quad (30)$$

where the adiabatic sound-speed gradient γ_A , the internal wave displacement scale ζ_0 , and the reference buoyancy frequency n_a are the input parameters.

vertical correlation length:

The vertical correlation length of internal waves is defined as follows:

$$L_v = \frac{n_0 B}{\pi n(z)} [M_j^{-1}]^{\frac{1}{2}} \quad (31)$$

The derivation of this result is presented in [1, 9].

4.4.2 Quantities at range of receiver:**ray depth:**

z coordinate of the point on the ray which has horizontal x coordinate equal to the range between the source and receiver.

ray angle:

The angle of inclination with respect to the horizontal of the acoustic ray at the range of the receiver.

travel time

The time interval needed for a sound signal from the acoustic source to travel along the ray to reach the receiver range. The calculation uses Snell's Law[1]:

$$tt = \frac{C(z_s)}{\cos \Theta_0} \int dx / C^2(z_{ray}(x)) \quad (32)$$

number of loops:

Number of double-loops in the range between the acoustic source and receiver.

$$n = [R/R_D] \quad (33)$$

caustics:

We find locations of caustics of rays by looking for zeros of $S_1(x)$.

rfrac = amod (rfinal, rmax):

$$R = R_D \cdot n + rfrac \quad (34)$$

Where R is the range between the source and receiver, R_D is the double-loop length, n is the number of loops between the source and receiver.

ray tube functions S_1, S_2 :

Values of these ray tube functions at the receiver range.

transmission loss (dB):

Transmission loss in the geometrical optics approximation.

$$tl = -10 \log_{10} |S_1(R)R| \quad (35)$$

4.5 Wave Propagation Region

The sound transmission is affected by propagation through a fluctuating ocean. The characteristic scales of sound-speed fluctuations are described by the

strength parameter Φ and the diffraction parameter Λ . The regions of different sound fluctuation behavior can be defined in terms of regions in $\Lambda - \Phi$ space[1, 9].

The saturated region is the region of the sound fluctuation ($\Lambda - \Phi$) diagram where a large number of micropaths are generated; the unperturbed ray is breaking into many rays. In the fully saturated regime these new rays are spread vertically over a region larger than a correlation length L_v , this is the region $\Phi > 1, \Lambda\Phi > 1$; in the partially saturated regime they are spread over a region smaller than L_v , this is the region $\Lambda\Phi > 1, \Phi \leq 1$. The paths that are separated by less than L_v have some correlation with each other; the paths separated by more than a correlation length are statistically independent.

The strength parameter, Φ , can be expressed as

$$\Phi^2 = q_0^2 \int_0^R dx \langle \mu^2(z_{ray}) \rangle L_p(\theta, z_{ray}) \quad (36)$$

so each increment in range (dx) contributes to the strength of the signal fluctuations an amount proportional to the variance of μ at this point of the ray and to the correlation length of the sound speed fluctuations along the direction of the ray at that point L_p [9, 5].

The diffraction parameter, Λ is a weighted average along the ray of $(R_F/L_v)^2/2\pi$, where R_F is the Fresnel zone radius and L_v is the vertical correlation length. This quantity is given by

$$\Lambda = \frac{q_0^2}{\Phi^2} \int_0^R dx \langle \mu^2(z_{ray}) \rangle L_p(\theta, z_{ray}) |g(x, x)| / (qL_v^2) \quad (37)$$

Λ is an integral along the equilibrium ray, $g(x, x)$ is the Green's function, q_0 is acoustic wave number.[5]

lambda phi, lambda phi square:

$$\Lambda\Phi, \Lambda\Phi^2$$

These Λ and Φ combinations are involved in definition of $\Lambda - \Phi$ diagram boundaries[1, 9] and in expressions for some of ocean fluctuation parameters.

ln (phi):

$\ln \Phi$ is needed for calculation of time, frequency, space separation scales and the microray focusing parameter γ .

4.6 Space Scales

vertical coherence length:

The vertical coherence length of the acoustic field z_0 which appears in (3) is defined by:

$$z_0^{-2} = q_0^2 \ln \Phi \int_0^R dx \langle \mu^2 \rangle L_p \{k_v^2\} [\xi_1(x)]^2 \quad (38)$$

where q_0 is acoustic wave number, $\{k_v^2\}^{1/2}$ is an appropriately averaged internal-wave vertical wave number, $\langle \mu^2 \rangle$ is the variance of sound-speed fluctuations L_p is sound-speed fluctuation correlation length along the ray tangent and $\xi_1(x)$ is the ray-tube function.[10] Note that $\{k_v^2\} = L_v^{-2}$

rms vertical-angle spread:

This quantity can be interpreted as an rms vertical arrival angle variation θ_v .

$$\theta_v = \frac{1}{(q \cdot z_0)} \quad (39)$$

where z_0 is the vertical coherence length and q is acoustic wave number.[10]

horizontal coherence length:

$$D(\Delta y_r) = 2q_0^2 \int_0^R dx \langle \mu^2(z_{ray}) \rangle L_p f(z, \theta; \Delta y') \quad (40)$$

$$\Delta y' = \Delta y_s + \frac{x}{R} (\Delta y_r - \Delta y_s) \quad (41)$$

and Δy_s and Δy_r are horizontal separation variables at the source and receiver, respectively.[10] Evaluation of D for general Δy_s and Δy_r could be used to calculate quantities of interest for moving sources. For most purposes it would be sufficient to set $\Delta y_s = 0$ and $\Delta y_r = 1$ km (see below).

decorrelation function f is given by:

$$f(z, \theta; \Delta y') = \left(\frac{(\Delta y')^2}{(\Delta y')^2 + (y_h)^2} \right)^{3/4} \quad (42)$$

$$y_h = L_h(\omega_i/\omega_L) \quad (43)$$

Where L_h is empirical length set to 12 km.

The phenomenological rms spread in horizontal angle is defined by [10]

$$\theta_h = [D(\Delta y_r)]^{1/2} / (q_0 \cdot \Delta y_r) \quad (44)$$

Note that θ_h is the apparent wavefront tilt measured by two receivers Δy_r apart. If Δy_s is always much less than y_h (for example, if $\Delta y_s = 0$ and $\Delta y_r = 1$ km) then

$$D(\Delta y) = (\Delta y / y_0)^{3/2} \quad (45)$$

Where the horizontal correlation length y_0 , which appears in (4), is defined by:

$$y_0^{-3/2} = 2q_0^2 \int_0^R dx \langle \mu^2 \rangle L_p \left[\frac{x}{R} + \frac{\Delta y_s}{\Delta y_r} \left(1 - \frac{x}{R}\right) \right]^{3/2} y_h^{-3/2} \quad (46)$$

and the rms horizontal-angle spread is approximately

$$\theta_h = (\Delta y_r q_0^4 y_0^3)^{-1/4} \quad (47)$$

4.7 Frequency Scales (Coherent Bandwidth)

The quantities τ_1 and τ_0 of (6) are calculated as follows [4, 11, 10]:

$$\tau_1 = \frac{\ln \Phi}{2C_0} \int_0^R dx \langle \mu^2 \rangle L_p \{k_v^2\} g(x, x) \quad (48)$$

transverse correlation of internal wave
if they wobble about coherent wave
if they wobble about coherent wave
longer
if it is
big value for τ_1

$$\tau_0^2 = \frac{1}{2} \left(\frac{\ln \Phi}{C_0} \right)^2 \int_0^R dx \langle \mu^2 \rangle L_p \{k_v^2\} \cdot \int_0^R dx' \langle \mu^2 \rangle L_p \{k_v^2\} \cdot [g(x, x')]^2 \quad (49)$$

$g(x, x')$ is defined in (15). $1/\tau_0$ is the coherent bandwidth.

4.8 Time Scales

pulse rms travel time τ :

The quantity τ is the rms deviation of the travel time from the value it would have if there were no internal wave fluctuation in the ocean. The coherence function for small frequency separation [eq.32] depends on τ [5, 10]:

$$\tau^2 = C_0^{-2} \int_0^R dx \langle \mu^2(z) \rangle L_p(\theta, z) = (\Phi/\sigma_0)^2 \quad (50)$$

field coherence time t_0 :

$$t_0^{-2} = q_0^2 \int_0^R dx \langle \mu^2 \rangle L_p\{\omega^2\} \quad (51)$$

where $\{\omega^2\}^{1/2}$ is an appropriately averaged internal-wave frequency that is dependent on local depth and position of the ray $z_r(x)$. [4]

t_0 is the effective overall acoustic phase time scale, appearing in (5).

Φt_0 is the effective internal-wave time scale.

intensity decoherence time t_I :

The intensity decoherence time t_I defined by (7) is calculated from [10]:

$$t_I^{-2} = q_0^2 \ln \beta_0 \ln \Phi \int_0^R dx \langle \mu^2 \rangle L_p\{k_v^2\} \{\omega^2\} \quad (52)$$

$$\cdot \int_0^R dx' \langle \mu^2 \rangle L_p\{k_v^2\} [g(x, x')]^2 \quad (53)$$

where

$$\ln \beta_0 = \begin{cases} \ln \frac{1}{2\Lambda\Phi \ln \Phi} & \text{if } \frac{1}{2\Lambda\Phi \ln \Phi} > e \\ 1 & \text{if } \frac{1}{2\Lambda\Phi \ln \Phi} \leq e \end{cases} \quad (54)$$

4.9 Validity of Path Integral

anisotropy:

validity frequency below which the theoretical treatment is not justified (weighted by Φ):

$$f_v(\Phi) = \frac{\int_0^R dx < \mu^2 > L_p^2 / (qL_v^2)}{\int_0^R dx < \mu^2 >^2 L_p} \cdot \sigma_0 \quad (55)$$

validity frequency for t_0 :

$$f_v(t_0) = \frac{\int_0^R dx < \mu^2 > L_p^2 \{\omega^2\} / (qL_v^2)}{\int_0^R dx < \mu^2 > L_p \{\omega^2\}} \cdot \sigma_0 \quad (56)$$

validity frequency for vertical separation:

$$f_v(z_0) = \frac{\int_0^R dx < \mu^2 > L_p^2 \{k_v^2\} \cdot [\xi_1(x)]^2 / (qL_v^2)}{\int_0^R dx < \mu^2 > L_p \{k_v^2\} [\xi_1(x)]^2} \cdot \sigma_0 \quad (57)$$

A quantitative estimate of the effect of inhomogeneity is given by ϵ_{inhom} average fractional change of the integrand in question over the height of the ray tube.

The validity parameter for the integrand used in calculating Φ is[10]:

$$\epsilon_{inhom}(\Phi) = \frac{\int_0^R dx < \mu^2(z_{rf}) > L_p(z_{rf}) - \int_0^R dx < \mu^2(z_r) > L_p(z_r)}{\int_0^R dx < \mu^2(z_r) > L_p(z_r)} \quad (58)$$

where $z_{rf} = z_r(x) + [(2\pi/q_0)g(x, x)]^{1/2}$, $z_r(x)$ is the vertical coordinate of unperturbed ray at x , $g(x, x)$ is the Fresnel's zone radius at x .

The validity parameter for the integrand used in calculating t_0 is[10]:

$$\epsilon_{inhom}(t_0) = \frac{\int_0^R dx < \mu^2(z_{rf}) > L_p(z_{rf}) \{\omega^2(z_{rf})\}}{\int_0^R dx < \mu^2(z_r) > L_p(z_r) \{\omega^2(z_r)\}} - 1 \quad (59)$$

The validity parameter for the integrand used in calculating z_0 is:

$$\epsilon_{inhom}(z_0) = \frac{\int_0^R dx < \mu^2(z_{rf}) > L_p(z_{rf}) \{k_v^2(z_{rf})\} \cdot [\xi_1(x)]^2}{\int_0^R dx < \mu^2(z_r) > L_p(z_r) \{k_v^2(z_r)\} [\xi_1(x)]^2} - 1 \quad (60)$$

4.10 Microray Focusing Parameter

In terms of Garrett-Munk internal wave spectrum[2], the γ that appears in (8) is expressed by[5, 12]:

$$\gamma = 2q_0^2 \int_0^R dx \langle \mu^2 \rangle L_p \{P(j, x)\} \quad (61)$$

where $P(j, x)$ can be approximately expressed in terms of two functions of x , called α and β :

$$P(j, x) = (1 - \cos \beta j^2) \exp(-\alpha j^2) \quad (62)$$

and

$$\alpha = M_j \ln \Phi k_v^2 \int_0^R dx' \langle \mu^2 \rangle L_p k_v'^2 [g(x, x')]^2 \quad (63)$$

$$\beta = \frac{k_v^2}{q_0} g(x, x) \quad (64)$$

where $\langle \mu^2(z) \rangle$ is the variance of the internal wave sound speed fluctuations as a function of depth, $L_p(z, \theta)$ is the correlation length of sound-speed fluctuations at depth z along direction θ , $k_v = \pi j n(z)/n_0 B$, $n(z)$ is the buoyancy frequency at depth z , $k_v' = \pi j n(z')/n_0 B$, M_j is the constant sum defined by Eq. (23), $g(x, x')$ is the Green's function, $g(x, x)$ is the Fresnel's zone radius of the ray tube at x , j is the vertical mode number, q_0 is the reference wave number defined by Eq. (22) and j_* is the constant defined in 3.1.3.

$$\{P(j, x)\} \equiv M_j \sum_{j=1}^{\infty} \frac{P(j, x)}{j(j^2 + j_*^2)}. \quad (65)$$

For very small $\alpha < 10^{-3}$ we may do an asymptotic expansion to obtain

$$\{P(j, x)\} = \frac{1}{4} \frac{\beta^2}{\alpha}. \quad (66)$$

For $10^{-3} < \alpha < 10^{-1}$ we approximate the sum by an integral which is valid for small α :

$$\begin{aligned} \{P(j, x)\} \approx & \frac{M_j}{2j_*^2} \left[\frac{1}{2} \ln \left(1 + \frac{\beta^2}{\alpha^2} \right) + e^{\alpha j_*^2} E_i(-\alpha j_*^2) \right. \\ & \left. - \operatorname{Re} \left\{ e^{(\alpha+i\beta)j_*^2} E_i[-(\alpha+i\beta)j_*^2] \right\} \right] \end{aligned} \quad (67)$$

where $Ei(z) = \gamma_E + \ln(-z) + \sum_{j=1}^{\infty} \frac{z^j}{j \cdot j!}$, $|\operatorname{arg}(-z)| < \pi$, $\gamma_E = 0.57721\dots$ is Euler's constant, or

$$\begin{aligned} \{P(j, x)\} \approx & \frac{M_j}{2j_*^2} \cdot e^{\alpha j_*^2} \left\{ [1 - \cos(\beta j_*^2)] \gamma_E - \ln[\alpha^2 j_*^4 + \beta^2 j_*^4]^{1/2} \right. \\ & \cdot [\cos(\beta j_*^2) - e^{-\alpha j_*^2}] + (1 - e^{-\alpha j_*^2}) \ln(\alpha j_*^2) \\ & + \sin(\beta j_*^2) \arctan(\beta/\alpha) \\ & \left. + \sum_{j=1}^n \frac{(\alpha \cdot j_*^2)^j - (\alpha^2 j_*^4 + \beta^2 j_*^4)^{j/2} \cos[j(\arctan(\beta/\alpha) + \beta j_*^2)]}{j \cdot j!} \right\} \end{aligned} \quad (68)$$

where $n = 3$ for $10^{-3} < \alpha \leq 10^{-2}$; $n = 6$ for $10^{-2} < \alpha \leq 10^{-1}$; and for $\alpha > 10^{-1}$ we directly sum Eq. (55) with $P(j, x)$ expressed by Eq. (52) with a decreasing number of terms as α becomes large, from 6 terms for $0.1 < \alpha \leq 0.13$ to 1 term for $\alpha < 5$.

5 DESCRIPTION OF SHORT OUTPUT FILE

The following is an example of the short output file.

Θ_{source} trav.time	z_{min} TL	$x(z_{min})$ τ	z_{max} τ_0	$x(z_{max})$ τ_1	R_D $t_0\Phi$	Θ_{max} $t_I\Phi$	$z_{receiver}$ $\Lambda_1 f$	$\Theta_{receiver}$ Θ_h	RID Θ_v
-9.500	251.1	45160.0	2698.0	20850.0	48610.2	9.524	306.1	5.499	-133
2194.0986	120.54	9.845	26.391	-42.025	0.3937	0.0618	42.8747	0.3928	2.0094
-8.750	272.5	44250.0	2493.4	20300.0	47880.4	8.776	273.5	-0.763	-136
2194.4849	111.19	11.063	25.575	-40.039	0.4465	0.0858	21.7124	0.4082	13.889
-8.000	296.8	43470.0	2297.1	19810.0	47300.4	8.028	1152.1	7.361	-137
2194.7217	120.50	12.541	22.639	-35.482	0.5260	0.1331	39.9564	0.4101	1.4286
-7.250	324.8	42800.0	2107.7	19380.0	46830.1	7.281	2094.4	0.881	-139
2194.9255	111.65	13.713	28.251	-40.038	0.6177	0.1398	38.8284	0.3987	7.7704
-6.500	359.1	42210.0	1923.6	19030.0	46350.0	6.535	1449.1	-4.621	-140
2195.0977	119.07	14.229	19.222	-29.731	0.7248	0.2509	37.1907	0.3675	1.9240
-5.750	396.9	41490.0	1736.8	18700.0	45580.2	5.789	1715.3	-0.973	-142
2195.2644	116.25	13.732	33.552	-49.770	0.8283	0.1558	31.5690	0.3213	7.9760
-5.000	433.5	38560.0	1543.8	17320.0	42480.2	5.045	1404.9	2.442	-153
2195.8391	124.71	13.116	85.402	-134.803	0.9061	0.0640	22.5707	0.2877	2.3743
-4.250	465.8	36930.0	1380.8	16490.0	40870.2	4.303	1229.6	2.372	-159
2196.1123	118.92	13.405	22.395	-34.881	0.9999	0.2853	19.9245	0.2719	2.1258
-3.500	498.0	35220.0	1224.1	15620.0	39190.1	3.564	625.7	-3.429	-166
2196.3137	121.85	13.762	28.282	-44.280	1.0907	0.2675	19.0445	0.2599	1.3771
-2.750	532.2	33280.0	1074.7	14490.0	37580.1	2.833	998.4	1.457	-173
2196.4326	122.75	14.454	84.660	-133.477	1.1940	0.1117	21.4981	0.2513	2.8298
-2.000	576.8	29140.0	948.6	12710.0	32860.1	2.112	624.1	-1.853	-198
2196.6895	123.14	15.641	76.793	-121.021	1.3150	0.1599	23.4113	0.2477	1.9961
2.000	576.9	3730.0	949.0	20160.0	32865.8	2.115	698.1	2.098	198
2196.6870	123.73	15.635	77.567	-122.426	1.3150	0.1582	23.4725	0.2474	1.7635
2.750	532.3	4300.0	1075.3	23100.0	37600.8	2.836	1034.4	-1.063	173

2196.4341	121.17	14.456	76.960	-121.139	1.1927	0.1229	21.5832	0.2516	4.0522
3.500	498.0	3980.0	1224.1	23580.0	39198.9	3.564	719.6	3.562	166
2196.3140	122.06	13.762	28.637	-44.879	1.0908	0.2641	19.0918	0.2590	1.3050
4.250	465.8	3940.0	1380.9	24380.0	40874.6	4.303	1377.2	-0.380	159
2196.1250	109.08	13.422	24.210	-1.100	0.9985	0.2644	19.9819	0.2723	20.463
5.000	433.5	3920.0	1543.8	25160.0	42485.1	5.045	1535.1	-0.600	153
2195.8586	118.25	13.148	72.883	-113.118	0.9050	0.0752	22.6834	0.2883	10.487
5.750	396.9	4090.0	1736.8	26880.0	45584.8	5.789	1338.7	-4.082	143
2195.2800	122.86	13.788	39.401	-62.033	0.8274	0.1333	31.7233	0.3220	1.7401
6.500	359.1	4150.0	1923.6	27330.0	46359.8	6.535	528.7	-5.859	141
2195.0735	120.26	14.300	20.589	-32.089	0.7247	0.2355	37.3016	0.3681	1.4655
7.250	324.8	4040.0	2107.7	27450.0	46830.7	7.281	1927.7	-3.183	139
2194.9629	115.04	13.788	12.590	-17.860	0.6175	0.3174	38.9449	0.3998	3.5159
8.000	296.8	3840.0	2297.1	27490.0	47304.9	8.028	1984.2	4.305	138
2194.7209	118.28	12.613	23.921	-37.294	0.5252	0.1269	40.0739	0.4111	2.3460
8.750	272.5	3640.0	2493.4	27580.0	47886.1	8.776	1228.1	8.016	136
2194.4612	121.22	11.102	23.306	-36.679	0.4464	0.0946	40.1856	0.4061	1.3412
9.500	251.1	3460.0	2698.0	27770.0	48618.8	9.524	1458.9	8.309	134
2194.0596	122.37	9.898	26.790	-42.239	0.3936	0.0613	43.2516	0.3929	1.2937

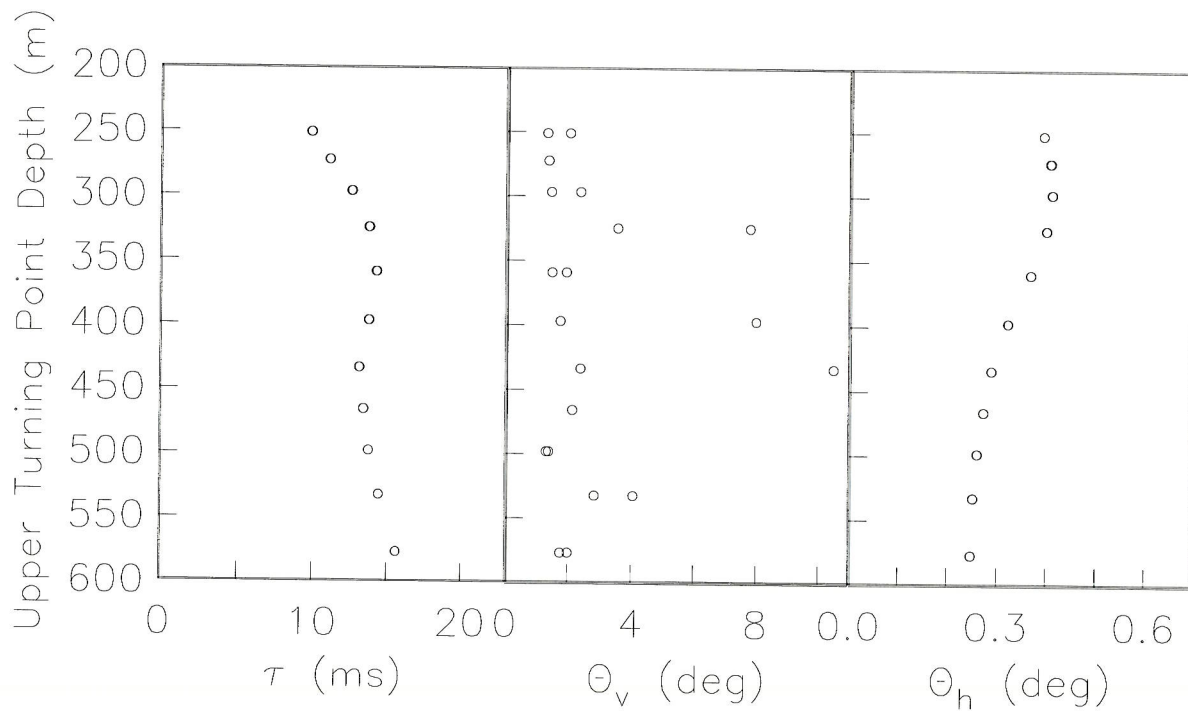


Figure 3: The three quantities plotted are the rms travel-time (τ), the vertical coherence angle (Θ_v), and the horizontal coherence angle (Θ_h). This plot was made from the information contained in the short output file listed above.